# MODELLING AIRBORNE BRAKE WEAR PARTICLE TRANSPORT IN SUBWAY SYSTEMS: A LINE-SCALE FRAMEWORK

Rodrigo Herrero, Carla Sánchez, Laura Rodríguez

*Metro de Madrid (MdM), ES*

DOI 10.3217/978-3-99161-087-8-037 (CC BY-NC 4.0)


## ABSTRACT

Subway systems present specific challenges for indoor air quality and associated health risks. Stations, platforms and tunnels constitute enclosed or semi-enclosed environments characterized by complex airflow patterns. This paper proposes a one-dimensional advection–diffusion transport model to represent the evolution of pollutants generated by mechanical braking along an entire subway line (Line 1 in Metro de Madrid). The formulation incorporates source terms, deposition (sink) mechanisms, detailed station and track geometry, the real dynamics of moving trains, the configuration of ventilation shafts, and time-dependent forced-ventilation operating schedules. The model makes it possible to proportionally quantify the spatial and temporal distribution of pollutant emissions resulting from the different mass-transport mechanisms involved in this environment, and it also enables the prediction of accumulated total values under various operating conditions. This framework enables comparative evaluation of different mitigation strategies aimed at reducing the impact of particulate emissions on air quality, with particular emphasis on assessing on board retrofit filtration systems designed by Tallano technologies to reduce pollutant mechanical brake generation at the source, beyond the conventional strategies of ventilation control and cleaning programs.

*Keywords:Railway Mechanical Braking, Subway Air Quality, On-board Brake Filtration*

## 1. INTRODUCTION

Over the past two decades, the improvement of air quality has become firmly established as one of the priority pillars of public health and urban sustainability policies. The growing social awareness of the effects of atmospheric pollution, together with the accumulated scientific evidence on its respiratory, cardiovascular, and neurocognitive impacts, has driven the deployment of monitoring programs, emission reduction plans, and increasingly stringent regulatory frameworks [1]. Among regulated and emerging pollutants, particulate matter (PM) occupies a central place due to its ability to penetrate the respiratory system, its high specific surface area that promotes the adsorption of toxic compounds, its compositional heterogeneity, and its robust relationship with morbidity and premature mortality [2].

In urban environments, underground infrastructures—and particularly subway systems—present specific challenges for indoor air quality. Stations and tunnels constitute enclosed volumes where airflow patterns are governed by geometry, ventilation regimes, and the piston effect induced by train movement, as well as by interactions with the outdoor environment through entrances and air intakes. In addition to the inletting of outdoor pollutants, there is

significant internal generation associated with wheel–rail contact, mechanical braking processes, catenary–pantograph interactions, the off-service operation of auxiliary diesel vehicles, the resuspension of deposited dust driven by passenger movement and train passages [3]. As a result, PM concentrations in this environment often exceed those outdoors and exhibit pronounced space-time variations, being sensitive to station typology, tunnel geometry, ventilation modes, train frequency and speed, and cleaning protocols [4 - 6].

This context requires the development of quantitative tools capable of describing and predicting particle dispersion, to support the optimization of ventilation, cleaning, and emission control strategies, as well as the assessment of exposure levels for passengers and employees. In the case of Metro de Madrid, due to the scale of the system, the diversity of station typologies, the variability in tunnel depth and cross-section, and the operational regimes constitute an ideal testing framework. The possibility of extrapolating insights to other stations and lines reinforces the value of a scalable and replicable approach, with potential for technological transfer to other urban networks. Given the diversity of emission sources, each characterized by its own specific generation mechanism, it is of particular interest to analyse the emissions associated with rolling-stock circulation, and specifically those linked to the operation of mechanical braking systems that complement regenerative braking in railway environments.

During peak hours, the high train density and the continuous acceleration–braking cycles resulting from short inter-station distances enhance the effectiveness of regenerative braking. However, the geometric constraints associated with platform stopping points require the final approach to stations to be supplemented with mechanical braking. Conversely, during off-peak hours, the available windows for energy exchange between trains are reduced, leading to increased reliance on mechanical braking systems. Emissions generated by mechanical braking processes consist primarily of Fe as the major component, along with trace metals characteristic of railway wear, such as Mn, Cu, Zn, Sb, Mg and Si, as well as significant fractions of elemental carbon and organic carbon [7]. Source apportionment studies based on single-particle analysis using SEM-EDX and on mass balance approaches indicate that wear particles associated with the braking system can account for approximately 15 to 24% of the PM10 mass in metro stations. Within this group, the emissions generated by brake pads and brake discs exhibit a particle size dependent distribution, as summarized in Table 1.

**Table 1:** Relative source contributions of brake-related components (pads and discs only) by particle size fraction, expressed in particle number and particle mass compared with other sources [7].

| Source | | Particle numbers (%) | | | Particle mass (%) | | |
|---|---|---|---|---|---|---|---|
| | | 1–10µm | 1 – 2.5µm | 2.5 – 10µm | 1–10µm | 1–2.5µm | 2.5 – 10µm |
| Brake wear | Discs | 3% | 2% | 5% | 5% | 3% | 6% |
| | Pads | 21% | 21% | 15% | 11% | 19% | 9% |
| Track -wheel | | 33% | 23% | 61% | 52% | 29% | 62% |
| Wire-pantograph | | 1% | 1% | 1% | 0.4% | 1% | 0.5% |
| Other external sources | | 39% | 49% | 16% | 30% | 45% | 21% |

Due to the complexity of the underlying generation process—dependent on the condition and typology of the railway braking components, especially pads, disc and wheel in case of tread units, as well as on train speed and process temperature—it is highly beneficial to rely on results obtained from dedicated test-bench experiments to quantify their magnitude as a source term.

For the development of the present study, data from pollution tests carried out on the UIC test bench of TU Graz were used, corresponding to commercial service of rolling stock operating on lines 5 and 10 of Metro de Madrid. These activities have been performed in the context of the EU-funded VERA project, which aims at developing retrofit systems for tailpipe and brake emissions from road and rail vehicles. On top of that, VERA expands to exposure studies, particularly within confined environments, such as the underground stations, and assesses the impacts on air quality and human health.

## 2. METHODOLOGY

### Mathematical model

The present study develops a one-dimensional space-time numerical model based on the advection-diffusion equation with time-dependent source terms. The model incorporates dynamic variability in the air velocity, associated with the train's piston effect and the forced ventilation system, as well as in the intensity of emissions linked to mechanical braking [8]. This formulation makes it possible to coherently represent the transients induced by railway operation and to capture the non-stationary evolution of the concentration along the tunnel-station domain.

### Simplifying assumptions

To reduce the complexity of the physical model and facilitate the numerical resolution of pollutant transport in the underground system, a series of simplifying assumptions are adopted based on typical metro operating conditions and on the spatial and temporal scales of interest [9]. The working fluid is the air contained within tunnels and stations, treated as incompressible and of constant density during the periods analyzed, managing mean velocity along each section. The flow is assumed to remain in a subcritical regime, without compressibility effects or the presence of shock waves, in accordance with the criteria established for ventilation modeling in underground transport systems [10]. It is also assumed that the pollutant is sufficiently well mixed throughout the medium (well-stirred model), because of the high Reynolds numbers and the resulting turbulence.

The mean airflow is approximated as one-dimensional and aligned with the longitudinal axis of the tunnel, neglecting lateral and vertical variations in velocity, concentration, and pressure in comparison with variations along the main flow direction. Consequently, the suspended particle concentration represents an average value over the cross-section. The thermal and pressure properties of the air are considered uniform and slowly varying, so buoyancy effects induced by thermal or density gradients are negligible at the scales analysed [11]. Emission and deposition processes are represented through equivalent source and sink terms, without explicitly resolving aerosol microphysics. The combined action of forced ventilation and the piston effect induced by train movement is incorporated through a time-dependent mean air velocity. Instantaneous mixing within each tunnel or station cross-section is assumed, ensuring that the computed concentration corresponds to the spatial average consistent with mass conservation in a one-dimensional model [9].

### Governing equations

The set of equations used to model the phenomenon includes a transport equation for a scalar magnitude $u(x,t)$, which represents the average pollutant concentration $[ug/m^3]$ along the subway infrastructure described by a one-dimensional advection–diffusion equation into a domain $\Omega = \{(x,t) \in \mathbb{R}^2 : 0 \leq x \leq L,\ 0 \leq t \leq T\}$ [12] as follows:

$$\frac{\partial u(x,t)}{\partial t} + c(x)\frac{\partial u(x,t)}{\partial x} + k(x)u(x,t) - \frac{\partial}{\partial x}\left[D(x)\frac{\partial u(x,t)}{\partial x}\right] = F(x,t) \qquad (1)$$

Where $c(x)$ represents the airflow velocity averaged over each section $S(x)$; $D(x)$ corresponds to the longitudinal turbulent diffusivity; $k(x)$ represents the term accounting the deposition/resuspension mechanism of material onto/from the surface of the tunnels and stations and $F(x,t)$ is the volumetric particle source in this study associated with the generation of PM due to brake system wear of each entire train moving along the line.

To model the air flow dynamics, the conservation equations of mass and momentum for incompressible flow at high Reynolds numbers are considered, including the arrangement of ventilation shafts along the line. So $\Omega$ is divided into adjacent characteristic subdomains, representative of station sections, tunnel segments, and compensation, supply, or extraction vents:

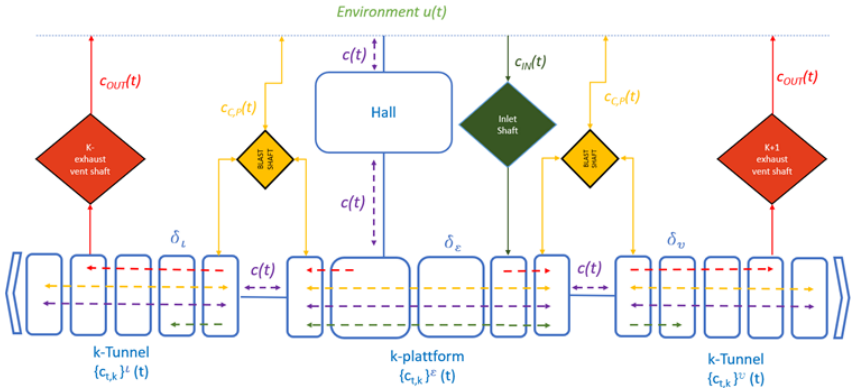


**Figure 1:** Schematic representation of a typical subway alignment section.

The operation of the forced-ventilation system consists of supplying fresh air through the fans installed in the shafts located at the stations and exhausting it to the outside through the fans installed in the shafts located inside the tunnels. In addition, there are compensation vents that regulate pressure imbalances and dampen the pressure waves associated with train movement.

To account for the flow induced by train motion, the velocity term $c(x)$ is transformed into a temporal coordinate, $c(t)$, train velocity $v_{train}(t)$ along the domain. By assembling these contributions for the set of $s$-th subdomains contained in the model, the following expression is obtained:

$$\rho\left\{\boldsymbol{\theta}\frac{\partial c(t)}{\partial t}\right\}_s = \left\{\boldsymbol{\omega}(\theta, f, g, c(t), v_{train}(t), x_{shaft})\right\}_s \quad (2)$$

Where $\boldsymbol{\theta}$ is a geometric factor that accounts for both train and infrastructure parameters—such as the train's frontal area $S_t$[m²], train length $l$[m], tunnel or station length $L$, and the cross-sectional area distribution $S(x)$. Its value depends on the presence (or absence) of trains within each $s$-th subdomain at time $t$. The term $\boldsymbol{\omega}$ represents the aggregated pressure-gradient contributions $\sum \Delta p_s$associated with train motion and airflow through tunnels, shafts, and stations. These contributions are determined by friction factors $f$, gravity $g$ (track gradient), train velocity $v_{\text{train}}(t)$, shaft locations $x_{\text{shaft}}$, and the mean flow velocity $c(t)$ within each $s$-th subdomain.

At $t = 0$, an air-velocity field is imposed because of the operation of the forced-ventilation system, with no train motion, such that $c(x,0) = C_0(x)$, varying with the cross-section $S(x)$in each segment. Likewise, an initial pollutant distribution is assumed, $u(x,0) = h(x)$. As boundary conditions, atmospheric pressure is prescribed at the locations of each compensation vent. At the tunnel endpoints, $x = 0$ and $x = L$, the pressure gradients produced by the fans in the shafts are imposed, $\Delta p_{x\,shaft}$ and a temporal pollutant distribution is assigned at the

inlet and outlet stations, corresponding to the departure and arrival stations, respectively, such that $u(0,t) = Z_0(t)$ and $u(L,t) = Z_L(t)$. So, the strong formulation of the model is completed with this set of boundary conditions.

### Numerical implementation

The implemented procedure consists of first solving the velocity $c(t)$ and pressure $p(t)$ fields from (2) using non-linear hydraulic impedance method [13] through different sub-domains by numerical approach. Once $c(t) \rightarrow c(x)$ is obtained, equation (1) is solved using an explicit finite-difference scheme on a regular spatial grid of $N_x$ nodes and a uniform time step. Spatial derivatives are discretized using a first-order upwind scheme for the advective term and a second-order centered difference approximation for the diffusive term. The upwind formulation ensures correct physical propagation of the scalar field in the direction of the airflow and prevents non-physical oscillations, while the centered discretization of diffusion provides a balanced representation of longitudinal mixing. The time step is determined according to classical stability criteria for both advection and diffusion, satisfying the Courant–Friedrichs–Lewy (CFL) condition and the standard diffusion stability constraint to avoid numerical instability or dispersion errors due to insufficient discretization.

$$\Delta t \leq \ min\left(\frac{CFL\,\Delta x}{c_{max}}, \frac{\Delta x^2}{2\,D}, \frac{2\,D}{c^2}\right) \quad (3)$$

## 3. PARAMETER ESTIMATION

### Deposition term $k(x)$

$k(x)$ represents the settling constant of airborne PM. This coefficient captures the combined effects of gravitational settling and residual removal processes under low-ventilation conditions. It was estimated using data from the blackout of April 28th, 2025, which temporarily halted both railway traffic and ventilation systems, while the battery-powered air-quality monitoring devices continued recording. This exceptional situation created a period with an almost complete absence of source emissions and particle resuspension, allowing PM concentrations to decay naturally over a much longer interval than the usual 4-hour service shutdown between 2 a.m. and 6 a.m. each day. The temporal evolution of PM levels was fitted using an exponential decay model, from which an effective first-order removal coefficient was derived. Measurements were obtained using calibrated monitoring devices compliant with the UNE 17660-1:2022 standard.

### Diffusion term $D(x)$

$D(x)$ is the turbulent diffusivity [$m^2/s$] representing the longitudinal mixing induced by train movement and ventilation within the tunnel. In this study, it is treated as an effective parameter that aggregates the turbulent dispersion processed unresolved in the model. Its magnitude was selected based on values reported in experimental studies and Computational Fluid Dynamics (CFD) simulations of railway tunnels, where it typically ranges between 0.1 and 0.8 $m^2/s$ under induced ventilation conditions [10].

### Source term $F(x,t)$

To quantify the source term associated with mechanical braking processes, we used the results of the tests carried out on the UIC dynamometric test bench at the Technical University of Graz, using railway equipment supplied by Metro de Madrid, together with an innovative retrofit emission-reduction system developed by Tallano technologies, capable of suctioning and filtering a large fraction of brake-generated particles before they disperse into the railway

environment. The tests enabled the characterization of emissions as a function of parameters such as train speed and applied braking effort, for different railway braking system configurations—TBU (tread brake unit) and DBU (disc brake unit)—tested both with and without the retrofit system.

**Figure 2**: From Left to right, original DBU pad, modified DBU pad, modified DBU pad holder, modified TBU sole.

This experimental characterization allowed the parametrization of the source term $F(x,t)$ referred to in (1), taking into consideration the specific braking configuration of the trains operating on the modeled metro line, which consist of six-car trainsets with three motor cars and three trailer cars, equipped with DBU systems on the 12 axles of the motor cars and TBU systems on the 24 wheels of the trailer cars. For the purposes of this study, reference is made to the PM2.5 granulometry in order to compare it with measurements recorded by the monitoring equipment installed in the network.

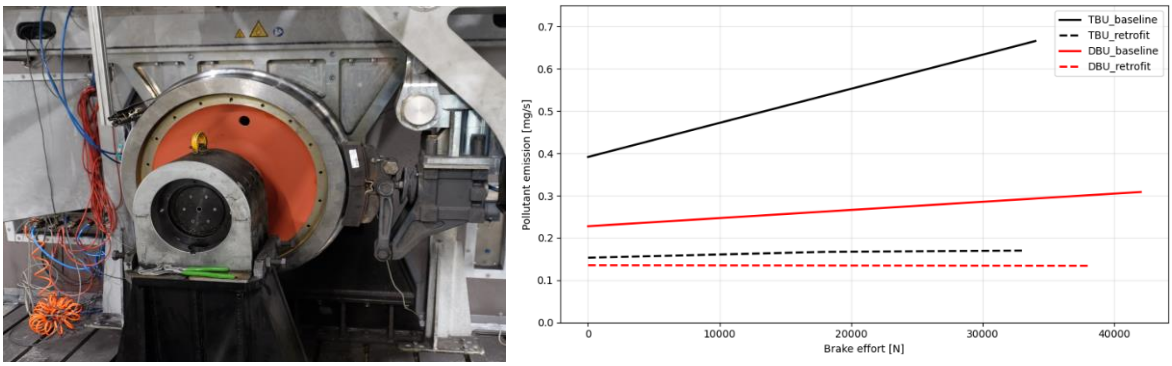


**Figure 3:** Arrangement of tread brake unit (TBU) on wheel rim in the test bench (left). Emission results according to the tested configurations (DBU, TBU, with/without retrofit system) (right).

## 4. RESULTS AND DISCUSSION

This section presents the results of the numerical simulations conducted to assess airborne, settled and exhausted to outdoor pollutant dynamics generated by brake emissions in different segments on Line 1 of Metro de Madrid.

Line 1 is the oldest line of the Madrid Metro, inaugurated in 1919, and runs between Pinar de Chamartín and Valdecarros, crossing the city diagonally from the North to the Southeast. It spans approximately 24 km/way of narrow-gauge tunnel and includes 33 stations/way. The total round-trip travel time (complete cycle on both tracks, way I and II) is 119 minutes. Line 1 crosses key central districts such as Sol, Gran Vía, and Atocha, forming a major north–

southeast axis of the city. It is one of the busiest lines in the network, carrying over 112,6 million passengers in 2025, up to 15% of the entire net. During peak hours, the line is operated with up to 38 six-car 2000 series trains (the oldest currently in operation), with headways of under 3 minutes.

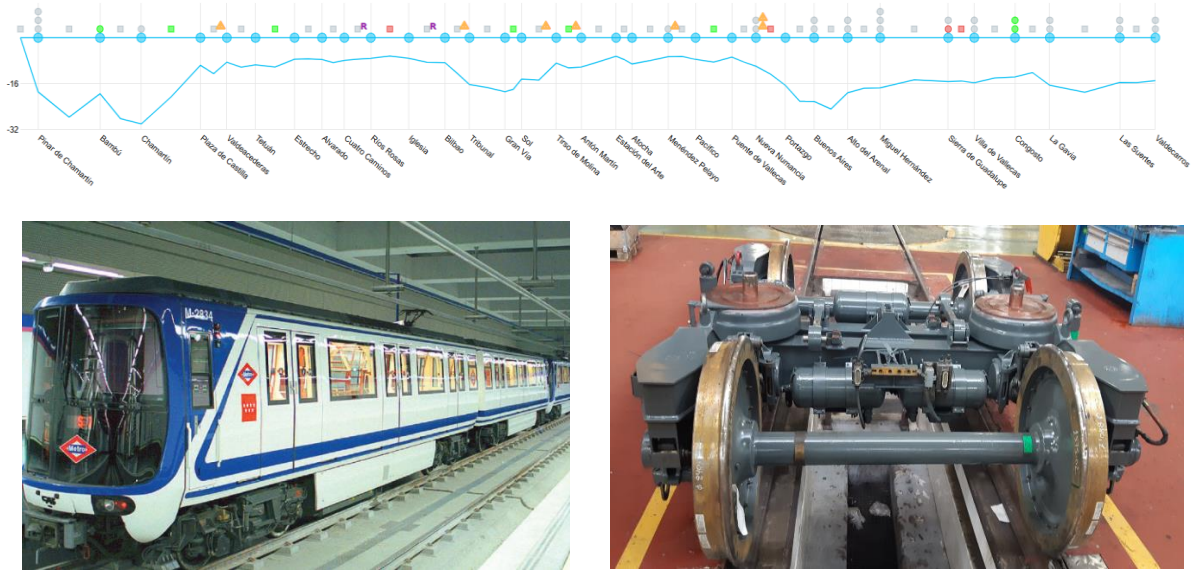


**Figure 4**: Track profile (upper); 2000-series operated on L1(left); bogie configuration (right).

This line is particularly relevant for the purposes of this study because the rolling stock operating on it is equipped with a mechanical braking system that combines both DBU and TBU technologies. Additionally, since half of the cars in each train consist of non-motorized trailers, the proportion of recoverable regenerative braking (75%) is lower than on other lines with more modern or more highly motorized trains (up to 85-90%). This results in a higher reliance on mechanical braking and therefore increases the significance of this line for the present analysis.

The Line 1 tunnel is equipped with pressure-compensation shafts located at both ends of each station, as well as extraction shafts equipped with axial fans in the mid-tunnel sections between stations. The layout of these shafts has been incorporated into the model to properly parametrize airflow patterns— and therefore the relevance of the convective transport terms — as well as to quantify the amount of pollutants exhausted through the ventilation shafts.

First, pollutant concentration is evaluated under four operational scenarios defined by the relative position of a second train. Figure 5 shows the resulting space–time concentration fields for the Estrecho–Alvarado segment, a short interstation characterized by high operating speeds. In the single-train reference case (Fig. 5a), the pollutant plume follows a predominantly advective pattern, with maximum concentrations occurring near the final braking zone and a progressive longitudinal spreading governed by piston-induced airflow and turbulent diffusion. When the crossing occurs at the initial platform (Fig. 5b), the departing train enhances outward transport, elongating the plume and reducing local accumulation in the upstream section. In contrast, the tunnel-crossing scenario (Fig. 5c) generates the highest concentration levels and the widest dispersion region, as the interaction between the airflow fronts induced by both trains limits immediate evacuation and promotes temporary pollutant retention within the confine domain. Finally, when the crossing takes place at final platform (Fig. 5d), the departing train from final platform partially extract the plume generated by the approaching train, resulting in lower peak accumulation.

The analysis was extended to the La Gavia–Las Suertes segment, which is characterized by a longer travel distance, Figure 6. After comparison with the shorter segment previously analyzed, it is observed that the increased distance allows advective transport to act over a larger domain, while turbulent diffusion has more time to smooth concentration gradients before reaching the final platform. As a result, the plume appears more elongated and spatially distributed, particularly in the tunnel-crossing scenario, where the interaction between the airflow fronts induced by both trains affects a wider region of the tunnel. Overall, a greater interstation length amplifies the spatial footprint of the emission event and reduces the sharp localization of peak concentrations.

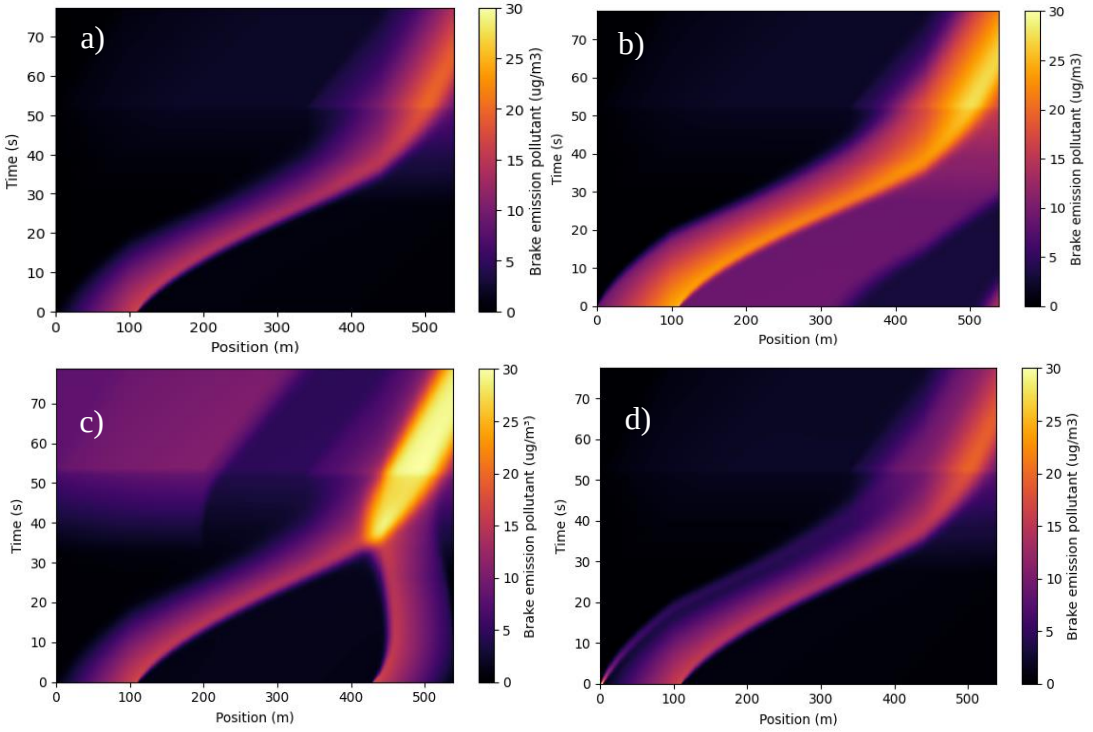


**Figure 5**: Spatial-temporal evolution of airborne pollutant concentration along the Estrecho–Alvarado segment (Way 1) under four operational scenarios: a) single train; b) crossing into initial platform; c) crossing inside tunnel; d) crossing final platform.

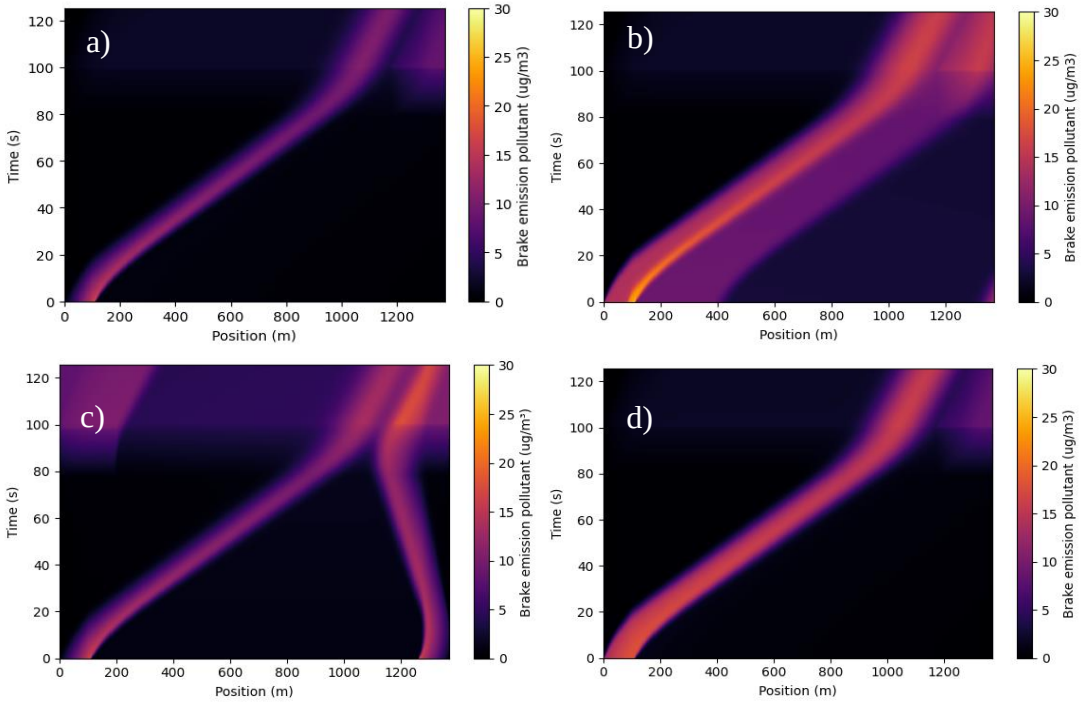


**Figure 6:** Spatial-temporal evolution of airborne pollutant concentration along the La Gavia -Las Suertes segment (Way 1) under four operational scenarios: a) single train; b) crossing into initial platform; c) crossing inside tunnel; d) crossing final platform.

In addition, the distribution of brake-emission pollutants accumulated over one hour of peak operation (38 trains/h) is analysed. The results quantify the fraction of emitted particles that remain airborne within the tunnel–platform domain, the fraction deposited on track and platform surfaces, and the fraction removed through ventilation.

Figures 7 show that the dominant fraction of pollutants generated by braking corresponds to particles deposited on track and platform surfaces, followed by the fraction remaining airborne, while the portion removed through ventilation is lower in both sections. The spatial distribution exhibits localized maxima that coincide with zones of higher braking demand, associated with descending gradients as well as geometric variations of the alignment. A correlation can be observed between the longitudinal gradient profile and the accumulation curves in Figure 8: segments with unfavourable slopes increase the need for pneumatic braking, thereby intensifying emissions and, consequently, the mass deposited and remaining airborne at those locations. The longitudinal redistribution of pollutants — both deposited and airborne — in the longer La Gavia–Las Suertes segment extends over a wider distance, indicating that the increased travel duration allows a more progressive dispersion of emissions.

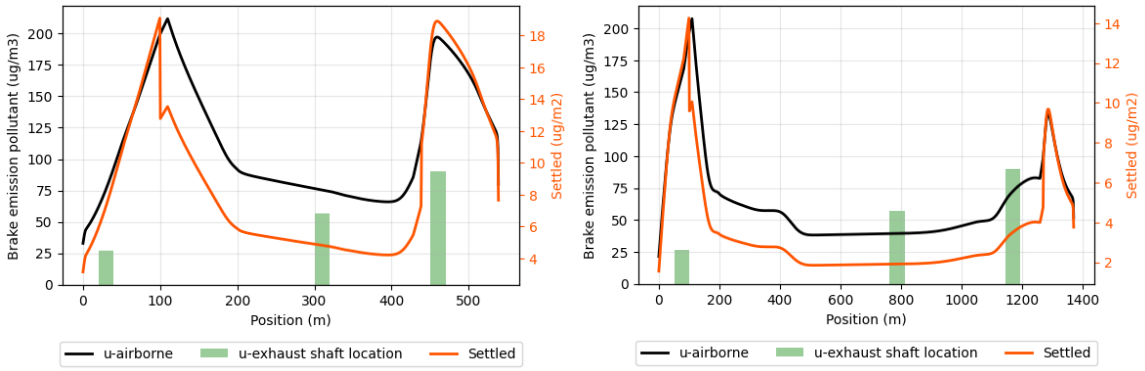


**Figure 7:** Airborne, settled on track–platform, outlet (exhaust) accumulated [1 h] pollutant during peak hour (38 trains interval 180 s): Estrecho–Alvarado section, Way I (left), and La Gavia -Las Suertes section, Way I (right).

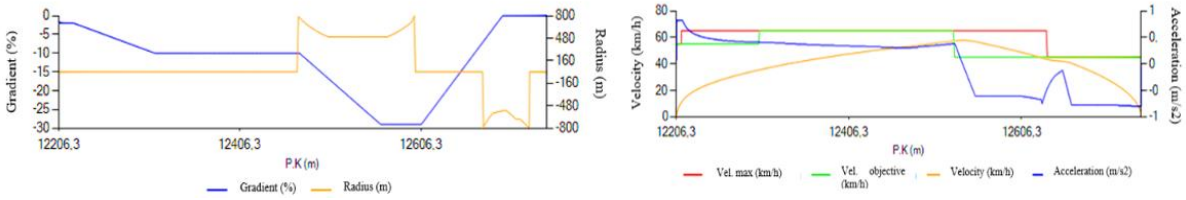


**Figure 8:** Example of longitudinal train dynamics profile Estrecho–Alvarado section, Way I.

To assess the impact of the retrofit system on emission dynamics, additional simulations were performed for the same segment under two configurations: conventional braking (baseline) and braking equipped with the Tallano retrofit device capable of suctioning and filtering a large fraction of brake-generated particles before they disperse into the railway environment.

The results clearly demonstrate a consistent reduction in emitted mass and peak concentrations when the Tallano retrofit system is implemented, underscoring the effectiveness of particle capture at the source and its direct impact on pollutant levels within the tunnel–platform environment (Figure 9). Overall, the net reduction approaches 70 % compared with the baseline scenario, highlighting the substantial mitigation potential of the system. These findings confirm that source-control technologies can play a decisive role in improving air quality in enclosed railway infrastructures.

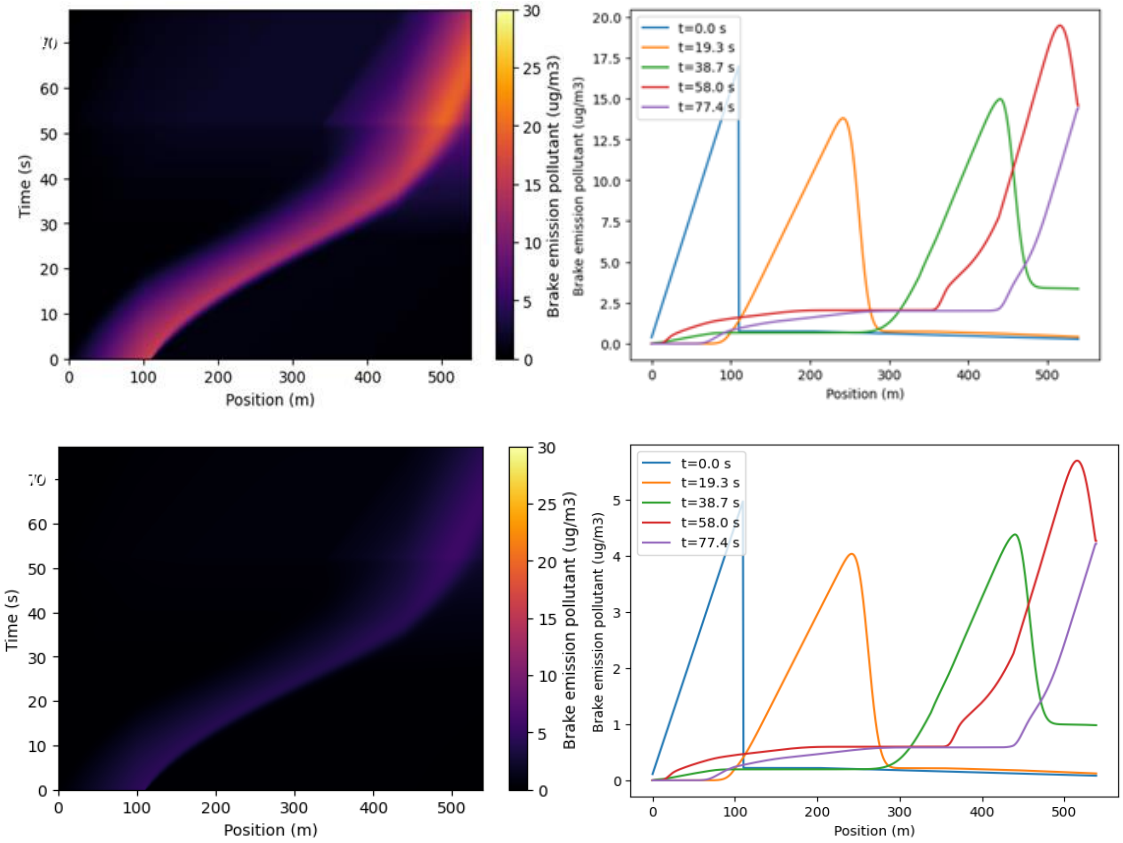


**Figure 9:** Spatial-temporal evolution of airborne pollutant concentration generated by brake emissions: a) Baseline and b) Retrofit system. Estrecho–Alvarado section, Way I.

Finally, Figure 10 shows the cumulative distribution of pollutants over one hour of operation for three cases: field measurements carried out using Class A air quality measurement devices at different Metro de Madrid locations (lines 8, 9 and 10), providing a realistic reference value; the model results under conventional configuration (without retrofit system); and the simulated case with the retrofit system activated. This comparison allows a direct contrast between numerical results and real data, as well as a quantitative assessment of the emission reduction associated with the implementation of the on-board filtration system. It should be noted that the measured in situ value encompasses the PM2.5 measured in the underground environment, including contributions from all potential sources (track–wheel interaction, wire–pantograph contact, external inputs, ancillary vehicles, infrastructure wear, among others). Since the developed model explicitly represents only the fraction associated with brake wear emissions (pads and discs), the experimental reference value has been proportionally adjusted according to the reported contribution of these components approximately 20% [7].

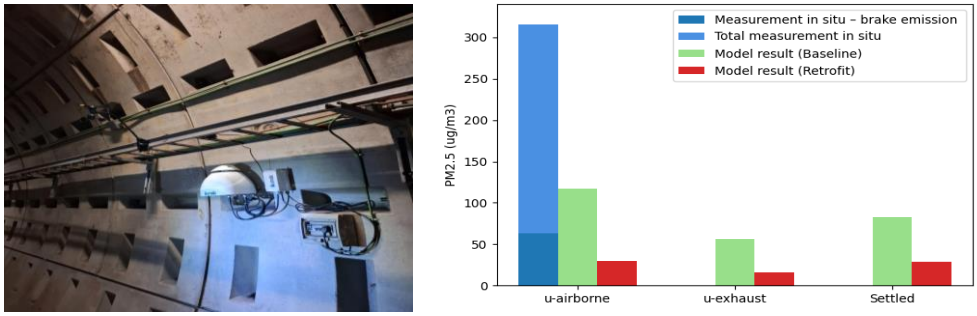


**Figure 10:** Comparative distribution airborne, settled on track–platform, outlet (exhaust) accumulated [1 h] pollutant during peak hour (38 trains interval 180 s).

In the case of Line 1, the trains have a higher proportion of motorized trains compared with trains running in Lines 8, 9 or 10, newer than L1 rolling stock), which implies a greater reliance on mechanical braking compared to the line where the in situ measurements were conducted. Consequently, the fraction of emissions attributable to brake wear is expected to be higher, which explains why the model results are greater than the experimentally measured values from other lines.

## 5. CONCLUSION

This study underscores the need for predictive tools capable of characterizing $PM_{2.5}$ dynamics generated by mechanical braking at the scale of an entire subway line under real operating conditions. The proposed one-dimensional transient framework integrates infrastructure geometry, ventilation shaft configuration, and can be parametrized for different forced-ventilation schedules, train intervals, and train dynamics within a simple yet physically consistent and computationally efficient formulation. This approach enables the representation of non-stationary pollutant transport and deposition processes in complex underground environments.

Comparison with measurement campaigns conducted at multiple locations along Metro de Madrid shows that the model reproduces the correct order of magnitude and captures the relevant spatiotemporal patterns, reinforcing its validity as a predictive tool despite the simplifying assumptions adopted. This experimental validation strengthens the robustness of the parametrization strategy and supports the physical coherence of the proposed formulation.

Beyond the evaluation of specific operational scenarios, the main contribution of this model lies in providing a scalable methodological platform for emissions assessment and for the evaluation of mitigation strategies—such as optimized velocity profiles that reduce pneumatic braking, enhanced cleaning protocols, improved ventilation schedules or the integration of onboard systems for emissions capture and filtration, such as the system tested and analyzed in this paper—at a network level. The model directly addresses a current need in the environmental management of metropolitan transit systems and establishes a foundation for further refinement, additional validation for other particle size fractions, and integration with exposure and health-impact assessment studies.

## ACKNOWLEDGEMENT

This work has been funded by the VERA project, which has received funding from the European Union's Horizon Europe research and innovation program under grant agreement No. 101056893.

## 6. REFERENCES

[1] Smith, J. D., Barratt, B. M., Fuller, G. W., Kelly, F. J., Loxham, M., Nicolosi, E., Priestman, M., Tremper, A. H., Green, D. C. "PM2.5 on the London Underground." Environment International, 134, 105188 (2020).

[2] Moreno, T., Pérez, N., Reche, C., Martins, V., de Miguel, E., Capdevila, M., et al. "Subway platform air quality: assessing the influences of tunnel ventilation, train piston effect and station design." Science of the Total Environment, 511, 711–722 (2014).

[3] Wang, X. (Richard), Gao, H. O. "Exposure to fine particle mass and number concentrations in urban transportation environments of New York City." Atmospheric Environment, 45(5), 1202–1211 (2011).

[4] Moreno, T., Pérez, N., Reche, C., Martins, V., de Miguel, E., Capdevila, M., et al. “Subway platform air quality: assessing the influences of tunnel ventilation, train piston effect and station design.” Science of the Total Environment, 511, 711–722 (2014).

[5] Nieuwenhuijsen, M. J., Gómez-Perales, J. E., Colvile, R. N. “Levels of particulate air pollution, its elemental composition, determinants and health effects in metro systems.” Science of the Total Environment, 377(1), 394–406 (2007).

[6] Querol, X., Moreno, T., Karanasiou, A., Reche, C., Alastuey, A., Viana, M., et al. “Variability of levels and composition of PM10 and PM2.5 in the Barcelona metro system.” Atmospheric Chemistry and Physics, 12, 5055–5076 (2012).

[7] VERA Project – Metro de Madrid. Technical Report 2025. Metro de Madrid, Madrid (2025).

[8] Zhang, X., et al. "Indoor air particulate matter concentration forecast for subway station platforms using a deep learning framework." Building and Environment, 2024.

[9] Gómez Giraldo, A., Álvarez-Villa, O.D., Monsalve, G., Vélez, J.I., & Blessent, D. (2017). Simulación del transporte de contaminantes en un medio subterráneo heterogéneo mediante el rastreo aleatorio de partículas. Aqua-LAC, 9(2), 15–32.

[10] Xu, X., Zhou, Y., Sun, H., Duan, X., & Wu, Y. (2010). A Model for Dispersion of Contaminants in the Subway. Tunnelling and Underground Space Technology, 2010.

[11] Fernández Gómez, C. (2004). Modelos matemáticos aplicables a los impactos ambientales. Consejería de Medio Ambiente, Región de Murcia.

[12] Coke, L. R., Sanchez, J. G., & Policastro, A. J. (2000). A model for the dispersion of contaminants in the subway environment (ANL/DIS/CP-101582). Argonne National Laboratory. U.S. Department of Energy. https://www.osti.gov/servlets/purl/755859

[13] Sajben, M. (1971). Fluid Mechanics of Train-Tunnel Svstems in Unsteady Motion. AIAA Journal, 9(8), 1538-1545

[14] HAWE Hydraulics, “Impedance Z,” 2024. https://www.hawe.com/es-es/fluid-lexicon/impedance-z/